Check for updates

Bacterial polyphosphates induce CXCL4 and synergize with complement anaphylatoxin C5a in lung injury

Julian Roewe[1], Sarah Walachowski[2], Arjun Sharma[1,2],
Kayleigh A. Berthiaume[2], Christoph Reinhardt[1]
and Markus Bosmann[1,2]*

[1]Center for Thrombosis and Hemostasis, University Medical Center Mainz, Mainz, Germany,
[2]Pulmonary Center, Department of Medicine, Boston University School of Medicine, Boston,
MA, United States

Polyphosphates are linear polymers of inorganic phosphates that exist in all living cells and serve pleiotropic functions. Bacteria produce long-chain polyphosphates, which can interfere with host defense to infection. In contrast, short-chain polyphosphates are released from platelet dense granules and bind to the chemokine CXCL4.

Here, we report that long-chain polyphosphates induced the release of CXCL4 from mouse bone marrow-derived macrophages and peritoneal macrophages in a dose-/time-dependent fashion resulting from an induction of CXCL4 mRNA. This polyphosphate effect was lost after pre-incubation with recombinant exopolyphosphatase (PPX) Fc fusion protein, demonstrating the potency of long chains over monophosphates and ambient cations. In detail, polyphosphate chains >70 inorganic phosphate residues were required to reliably induce CXCL4. Polyphosphates acted independently of the purinergic P2Y1 receptor and the MyD88/TRIF adaptors of Toll-like receptors. On the other hand, polyphosphates augmented LPS/MyD88-induced CXCL4 release, which was explained by intracellular signaling convergence on PI3K/Akt. Polyphosphates induced Akt phosphorylation at threonine-308. Pharmacologic blockade of PI3K (wortmannin, LY294002) antagonized polyphosphate-induced CXCL4 release from macrophages. Intratracheal polyphosphate administration to C57BL/6J mice caused histologic signs of lung injury, disruption of the endothelial-epithelial barrier, influx of Ly6G$^+$ polymorphonuclear neutrophils, depletion of CD11c$^+$SiglecF$^+$ alveolar macrophages, and release of CXCL4. Long-chain polyphosphates synergized with the complement anaphylatoxin, C5a, which was partly explained by upregulation of C5aR1 on myeloid cells. C5aR1$^{-/-}$ mice were protected from

polyphosphate-induced lung injury. C5a generation occurred in the lungs and bronchoalveolar lavage fluid (BALF) of polyphosphate-treated C57BL/6J mice. In conclusion, we demonstrate that polyphosphates govern immunomodulation in macrophages and promote acute lung injury.

Introduction

Inorganic polyphosphates (PolyP) are polymers of phosphate residues joined by high-energy phosphoanhydride bonds, which may be as short as three or as long as 1,700 residues *in vivo* (1, 2). Polyphosphates are ubiquitous and evolutionarily conserved, and previous studies have characterized both regulatory and chaperone functions beyond their original roles as phosphate and energy reservoirs (1, 3, 4). For a homopolymeric molecule, polyphosphates affect an astounding number of biological functions, including metabolic regulation through stimulation of mTOR (5), virulence and resistance to oxidative stress (6), regulation of complement activation (7), and blood clotting with polymer length-dependent effects in humans (2). Platelets typically produce polyphosphates with a size of less than 100 monomers long, whereas bacteria produce polyphosphates of several hundreds or more units (2).

Polyphosphates interfere with the differentiation and function of macrophages during bacterial infection (8–10). Polyphosphates prevent phagosome acidification and thus enhance survival of bacteria after phagocytosis by macrophages (8, 10). The MHCII-dependent antigen presentation machinery is suppressed by polyphosphates (8). LPS-primed macrophage polarization is skewed towards an M2-resembling phenotype characterized by suppression of NOS2 as a marker for M1 macrophages (8, 11). In addition, long-chain polyphosphates reduce LPS-induced STAT1 phosphorylation that is required for type I interferon production (8). Accordingly, the production of the type I interferon induced chemokine, CXCL10, is decreased by long-chain polyphosphates (8). The phagocytosis-induced release of CCL2 is blocked in macrophages (8). All these effects are specific to long-chain polyphosphates, which overwhelmingly antagonize beneficial host responses. On the other hand, short-chain polyphosphates (the length produced by platelets *in vivo*) enhance CXCL4 binding to *E. coli* and trigger neoepitope anti-CXCL4/polyanion antibody-mediated phagocytosis by polymorphonuclear neutrophils (PMNs) (12).

CXCL4, also known as platelet factor 4 (PF4), is a chemokine which binds polyanionic molecules like polyphosphates and others such as heparin, DNA, RNA, and lipid A (12). CXCL4 ligates with the CXCR3 receptor in mice and the CXCR3B splice variant in humans (13). CXCL4 plays regulatory roles in hemostasis/thrombosis, inflammation, angiogenesis and wound healing (14, 15).

Bacterial infections can lead to life-threatening complications such as sepsis, acute lung injury (ALI), and acute respiratory distress syndrome (ARDS). ALI/ARDS are severe respiratory conditions characterized by pulmonary edema, inflammation of the alveolar epithelium, and destruction of healthy lung tissue (16). ALI/ARDS and sepsis often co-exist in the same critically ill patients and have limited FDA-approved treatment options. We have recently reported that long-chain polyphosphates mediate death in *E. coli* sepsis and that targeting polyphosphates using recombinant exopolyphosphatase increases survival in mice (8). However, a pathogenic role of long-chain polyphosphates in ALI/ARDS has not yet been investigated. In contrast, numerous studies over recent decades have highlighted the critical role of the anaphylatoxin, C5a, in the pathogenesis of ALI/ARDS (17–19). C5a is a potent peptide generated during complement activation, which binds the C5aR1 receptor to directly promote chemotaxis of PMNs and to induce chemokines in myeloid cells (16). Intratracheal C5a administration to healthy mice is sufficient to unleash a robust inflammatory response similar to human ARDS (16).

Here, we identified the property of bacterial-type, long-chain polyphosphates to induce CXCL4 release from macrophages and during lung injury. The acute deleterious effects of polyphosphates in the lung were chain-length dependent and amplified by complement component C5a rather than by CXCL4.

Methods

Mice

All animal experiments were approved by the State Investigation Office of Rhineland-Palatinate and the

Institutional Animal Care and Use Committee (IACUC) of Boston University. All mice were housed in a 45-60% humidity, 22 ± 2°C ambient temperature, controlled light/dark (12 h/12 h) cycle, with free access to food and water. C57BL/6J mice (8-12 weeks old), C5aR1$^{-/-}$ mice, MYD88$^{-/-}$ mice, TRIF$^{-/-}$ mice, and P2Y1$^{-/-}$ mice (all on C57BL/6J background) were maintained in a specific pathogen-free environment. Sex-age matched cohorts were used for experiments.

Macrophages

Bone marrow-derived macrophages [BMDMs; purity: >95% F4/80$^+$CD11b$^+$ cells (18)] were generated by culturing mouse bone marrow cells with L-929 cell-conditioned medium for 7 days (18). Peritoneal-elicited macrophages (PEMs) were isolated 4 days after i.p. injection of 1.5 ml 2.4% (w/v) thioglycollate (Becton Dickinson, Franklin Lakes, NJ). The cultivation of macrophages was performed in RPMI 1640 (Thermo Fisher Scientific) supplemented with 100 U/ml penicillin-streptomycin (Thermo Fisher Scientific) and 0.1% (w/v) bovine serum albumin (Carl Roth, Karlsruhe, Germany) at 37°C, 5% CO_2, and 95% humidity.

Lung injury

Mice were anesthetized with ketamine/xylazine before surgical exposure of the trachea on an upright surgical stand (17). The following substances were slowly injected intratracheally (i.t.) in 40 µl phosphate buffered saline (PBS): Synthetic polyphosphates of the doses and chain-lengths as indicated in the figure legends, recombinant mouse C5a (500ng/mouse; R&D Systems, Minneapolis, MN, USA), and recombinant mouse CXCL4 (500ng/mouse; R&D Systems, Minneapolis, MN, USA). Sham treated mice received an equal volume of PBS i.t. alone. At the end of experiments (6-12 hours), mice were euthanized for collection of bronchoalveolar lavage fluid (BALF) and lungs. BALF were centrifuged to separate cells before further analysis or cryopreservation at -80°C.

Colorimetric assays

The CXCL4 ELISA kit was purchased from R&D Systems. The cell-free supernatants or cell-free BALF were analyzed according to the manufacturer's protocol. In short, samples were diluted in PBS supplemented with 0.1% BSA to fit into the standard range. Optical densities of oxidized TMB were measured with an Opsys MR Dynex microplate reader or a Tecan Infinite M Nano plate reader. No interference with optical density measurements was observed when long-/short-chain polyphosphates (50 µM) were added directly to rmCXCL4 of the ELISA standard curve.

Mouse albumin was quantified by ELISA (Bethyl Laboratories, Montgomery, TX, USA). Total protein was determined by BCA assay (Pierce, Rockford, IL, USA).

Flow cytometry

For surface staining, the cells were washed in ice-cold sterile PBS (650g, 5 min, 4°C) and stained for 30 min with fixable viability dye eFluor 780 (Thermo Fisher Scientific, 1:1000) using heat-killed (1 min, 65°C) cells as positive controls. Next, cells were washed twice with FACS buffer [1% (w/v) BSA, 0.01% (w/v) sodium azide, 2.5 mM EDTA in sterile PBS], preincubated for 20 min with anti-mouse CD16/CD32 antibody (TruStain FcX, BioLegend, San Diego, CA, USA, 1:50) in FACS buffer followed by 20 min incubation with fluorescent dye-conjugated, anti-mouse antibodies for CD11b (clone M1/70, 1:100), Ly6G (clone 1A8, 1:50), F4/80 (clone BM8, 1:100), CD11c (clone N418, 1:600), SiglecF (clone E50-2440, 1:400), or matched fluorochrome-labeled isotype antibodies (all from BioLegend).

For phospho-flow cytometry, cells were washed with FACS buffer after stimulation, fixed for 20 min with Cytofix (BD Biosciences), washed with FACS buffer, re-suspended in pre-cooled (-20°C) Perm III buffer (BD Biosciences) and incubated overnight at -20°C. Thereafter, samples were washed again with FACS buffer, incubated for 15 min on ice with anti-CD16/CD32 blocking antibody (clone 93, BioLegend, 1:50) before antibodies against phospho-Akt(T308) (clone J1-223.371, BD Biosciences, 1:10), CD11b and F4/80 antibodies were added for additional 30 min. The cells were washed with Perm/Wash and re-suspended in FACS buffer.

At least 50,000 events of interest were acquired on a FACSCanto II or LSR II (BD Bioscience). For cell counting, 123count eBeads (Thermo Fisher Scientific, 1:15) were added according to the manufacturer's instructions. FlowJo V10.0-V10.8.1 Software (FlowJo, Ashland, OR) was used for data analysis.

Reverse transcription and real-time PCR

Macrophages were lysed and total RNA was isolated using the RNeasy Mini Kit (Qiagen, Venlo, Netherlands). Reverse transcription of cDNA was performed with the High-Capacity cDNA Reverse Transcription kit (Life Technologies, Carlsbad, CA) in a Mastercycler pro S (Eppendorf, Hamburg, Germany). Quantitative PCR was performed on a C1000 with CFX real time PCR detection system (Bio-Rad Laboratories) using 1-2 ng cDNA per sample complemented with iQ SYBR$^®$Green Mastermix (BioRad) and specific forward and reverse primers at a concentration of 0.5 µM each. *Cxcl4* gene expression was compared between samples by normalizing to *Gaph* expression and applying the $2^{-\Delta\Delta Ct}$ formula (20). Primer sequences were as

follows: mouse *Gadph* 5'-TACCCCCAATGTGTCCGTCGTG-3' (forward), 5'-CCTTCAGTGGGCCCTCAGATGC-3' (reverse); mouse *Cxcl4* (NM_019932) 5'-CAGCTAAGAT CTCCATCGCTTT-3' (forward), 5'-AGTCCTG AGCTGCTGCTTCT-3' (reverse) (21).

Histology

Lungs were inflated with 500 µl of paraformaldehyde (4%) for fixation, and paraffin-embedded sections were stained with hematoxylin and eosin (H&E) in the histology core facility of the University Medical Center Mainz. An Olympus IX73 inverted oil immersion microscope with SC30 camera and Cell Sens Dimension V1 software was used for image acquisition (Olympus, Hamburg, Germany).

Bead-based phosphoprotein assay

The phosphorylation status of Akt was evaluated in lysed macrophage samples (Bio-Plex Cell Lysis Kit; Bio-Rad) using the phospho-Akt(Thr308) kit from Bio-Rad following the manufacturer's protocol. Phospho-Akt content reflecting fluorescence was measured in a Luminex-200/BioPlex-200 system (Bio-Rad) and normalized to fluorescence intensities of unstimulated control macrophages.

Immunoprecipitation and western blot

For C5a protein detection, the right lobes of each lung were homogenized and lysed in RIPA buffer containing protease inhibitors (Thermo Fisher Scientific). Equal volumes of fresh lung lysates (1 ml) and BALF samples (500 µl) were immunoprecipitated with polyclonal goat anti-mouse C5a antibodies (R&D systems, Minneapolis, MN) and protein A agarose beads (Thermo Fisher Scientific) as described previously (16). Proteins were separated by electrophoresis on 15% SDS-polyacrylamide gels (Bio-Rad Laboratories, Hercules, USA) under reducing conditions (i.e. in the presence of β-mercaptoethanol) and blotted onto polyvinylidene difluoride membranes. Blots were probed with polyclonal anti-mouse C5a antibodies and anti-goat IgG HRP-conjugated secondary antibody (R&D systems), were developed using chemiluminescent substrate (Thermo Fisher Scientific), and visualized with the ChemDoc imaging system (Bio-Rad Laboratories). The abundance of C5a in immunoprecipitated BALF or lung lysates from L-PolyP-treated mice was normalized relative to the abundance of C5a detected in sham control mice. Recombinant mouse C5a (R&D systems) was used as a positive control and PBS was used as negative control. Each control also contained protein A agarose beads, antibodies, and Laemmli buffer.

Reagents

Polyphosphates were a gift from Dr. James H. Morrissey and Dr. Stephanie A. Smith (see Kerafast #EUI002 and #EUI005 for further specifications). The modal chain lengths and distributions in terms of inorganic phosphate residues [P_i] were as follows: Short-chain polyphosphates (S-PolyP; P_i: ~70; range: 25–125 phosphates), medium-chain polyphosphates (M-PolyP; ~240 P_i; range: 150–325 phosphates), long-chain polyphosphates (L-PolyP; P_i: ~700; range: 200–1300+ phosphates) that were solubilized from high-molecular-weight polyphosphates as described before (22). PolyP preparations of narrow size distribution were prepared as described previously (2), and are indicated in Figure 1E by their polymer length followed by "mer" (e.g., 134mer). Lipopolysaccharide (Escherichia coli, serotype O111:B4) was purchased from Sigma-Aldrich. Wortmannin and LY294002 were obtained from Tocris Bioscience (Bristol, United Kingdom).

Recombinant PPX1-Fc and PPX1-D127N-Fc fusion proteins were expressed in *E. coli* as a customized project (Biologics International Corp, Indianapolis, IN, USA). Proteins were lyophilized after extensive dialysis against 1-fold PBS (pH 7.4), and reconstituted in sterilized water before use. The purity was >90% as judged by SDS-PAGE analysis and endotoxin was <1 EU/µg as determined by gel clot endotoxin assay. Protein sequences are available as Supplementary File 1.

Human single cell RNA-sequencing data analysis

The expression of CXCL4 and its receptor CXCR3 were assessed in an open access human lung transcriptome dataset to understand their cellular distribution. The human lung transcriptome dataset from Travaglini et al. (23) was comprised of normal uninvolved lung tissue from three patients undergoing lobectomy for lung cancer, which was sequenced after enzymatic digestion. The processed data from 10X Chromium sequencing with cell type (free) annotations was retrieved from cellxgene (24), re-normalized, and finally integrated using the Harmony (25) wrapper function in Seurat (26).

Statistical analysis

Statistical analysis and graphs were prepared in Prism v7-9 (GraphPad Software). Data in graphs are depicted as mean ± standard error of the mean (S.E.M.). *In vitro* experiments were repeated as 2-3 independent biological replicates and are shown as representative or pooled data. *In vivo* experiments were done with the numbers of mice per group as indicated by symbols
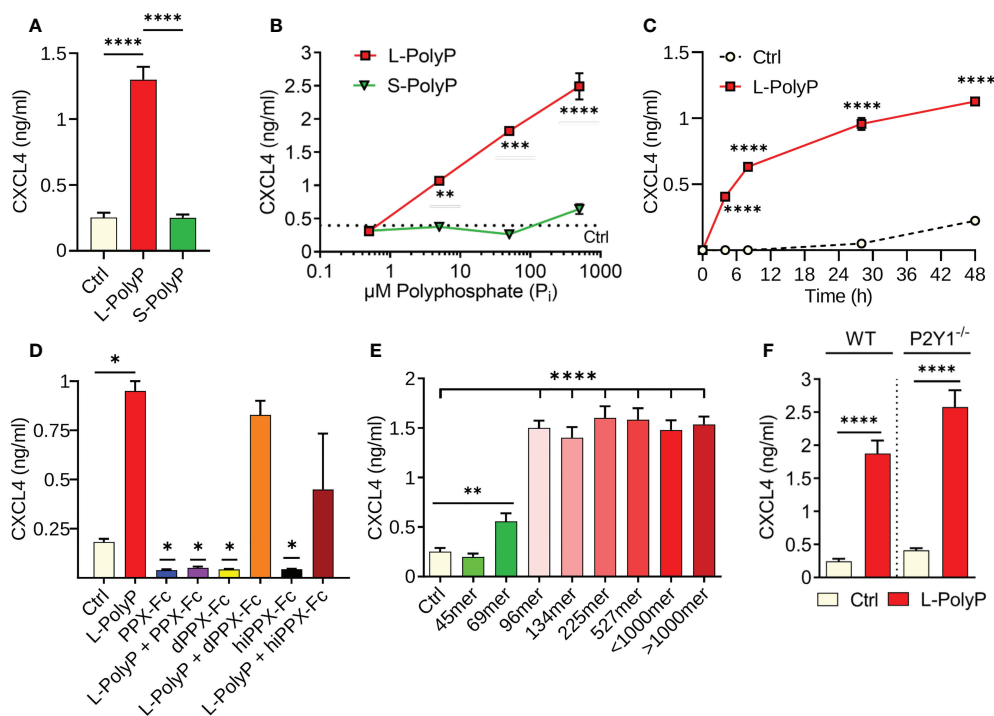
FIGURE 1

Polyphosphates induce CXCL4 release from macrophages. **(A)** CXCL4 in supernatants of bone marrow derived macrophages (BMDMs) from C57BL/6J wild type mice after incubation with long-chain polyphosphates (L-PolyP; P_i700, 50 µM) or short-chain polyphosphates (S-PolyP; P_i70, 50 µM) for 24 h. Resting macrophages served as controls (Ctrl). **(B)** Dose-response of CXCL4 release from macrophages (BMDMs) with different concentrations of long-chain or short-chain polyphosphates compared to basal levels from control macrophages, 24 h. **(C)** Time course of CXCL4 release from peritoneal elicited macrophages (PEMs) after long-chain polyphosphates (50 µM). **(D)** Long-chain polyphosphates (50 µM) were incubated overnight at 37°C with recombinant exopolyphosphatase-Fc fusion protein (PPX-Fc), mutated/dead exopolyphosphatase-Fc protein (dPPX-Fc), or heat inactivated exopolyphosphatase-Fc protein (hiPPX-Fc) followed by transfer to macrophages (PEMs) and CXCL4 detection after 24 h. **(E)** Polyphosphate polymers of narrow chain length distributions were incubated with macrophages (PEMs) followed by CXCL4 detection, 24 h. **(F)** CXCL4 induced by long-chain polyphosphates in macrophages (BMDMs) of wild type mice and P2Y1$^{-/-}$ mice, 24 h. CXCL4 was measured by ELISA for all experiments shown. Polyphosphate concentrations were 50 µM in all experiments except for frame B. All data are representative of 3 independent experiments. Data are presented as mean $\pm$ SEM; *$p < 0.05$; **$p < 0.01$; ***$p < 0.001$; ****$p < 0.0001$.

(circles, squares, triangles) in the figures. Two-group single comparisons were made with a two-tailed, unpaired Student's t-test. Multiple comparisons were made with a one-way or two-way ANOVA. P values <0.05 were considered significant.

Results

Long-chain polyphosphates induce CXCL4 in macrophages *via* PI3K/Akt signaling

In our screens and previous work using macrophages (8), polyphosphates alone did not induce cytokine/chemokine release (e.g., CCL2, CCL7, CCL9, CXCL10; data not shown) with the exception of CXCL4. To characterize the role of polyphosphates in inducing CXCL4 release, cultures of bone-marrow derived macrophages (BMDMs) from C57BL/6J wild

type mice were incubated for 24 h with long-chain (L-PolyP; mean polymer length of ~700 inorganic monophosphate residues [P_i]) or short-chain polyphosphates (S-PolyP; ~70 P_i). Long-chain polyphosphate-treated macrophage supernatants showed a substantial increase in CXCL4 concentrations compared to controls (resting macrophages), whereas short-chain polyphosphates had no observable effect (Figure 1A). Next, we investigated the kinetics of polyphosphate-mediated induction of CXCL4. Long-chain polyphosphates enhanced CXCL4 release in a dose- and time-dependent fashion from BMDMs and peritoneal macrophages (PEMs), respectively, while short-chain polyphosphates had no significant impact across the different concentrations (0.5-500 µM) and time points (0-48 h) tested (Figures 1B, C).

The amounts of polyphosphates are expressed as concentrations of monophosphate units, meaning that 50 µM of long-chain polyphosphates (P_i 700) contain 10-fold fewer chains than 50 µM of short-chain polyphosphates (P_i 70). Based

on our findings, 50 μM concentrations of polyphosphates at 24 h were considered as optimal conditions of strongest effect size and used for subsequent experiments with macrophages. No qualitative differences in the responsiveness to long-chain polyphosphates of either BMDMs or PEMs were noted (data not shown).

The long-chain polyphosphate effect on CXCL4 release was validated by incubating polyphosphates overnight at 37°C with recombinant exopolyphosphatase-Fc fusion protein (PPX-Fc), mutated/dead exopolyphosphatase-Fc protein (dPPX-Fc), or heat inactivated exopolyphosphatase-Fc protein (hiPPX-Fc), which were then transferred to macrophages for 24 h. As predicted, the activity of long-chain polyphosphates disappeared after exopolyphosphatase digestion. However, long-chain polyphosphates continued to induce CXCL4 in macrophages treated with non-functional exopolyphosphatases (dPPX-Fc, hiPPX-Fc; Figure 1D), confirming that polyphosphates have a direct and chain-length dependent effect on CXCL4 release. In another series of experiments using polyphosphate preparations with a more narrow range of chain lengths, we observed that polymers of ~100mer length onwards exert a maximal potency to induce CXCL4 release in macrophages after 24 h (Figure 1E).

Interaction of polyphosphates with the P2Y1 receptor was reported to amplify inflammatory signals in endothelial cells (27). Therefore, we assessed whether P2Y1 also modulates the effects of polyphosphates on CXCL4 release in macrophages through an experimental design involving macrophages from wild type (WT) and P2Y1$^{-/-}$ mice. P2Y1 did not appear to have any effect on long-chain polyphosphate-mediated CXCL4 release in macrophages (Figure 1F), suggesting that it is not required for the biological activity of polyphosphates in macrophages.

Toll-like receptor 4 (TLR4) is a key pattern recognition receptor that detects bacterial LPS and other PAMPs/DAMPs. TLR4 initiates inflammatory responses through the two adaptor molecules, MyD88 and TRIF, which are essential for all TLRs (28). Macrophages treated with a combination of long-chain polyphosphates and LPS showed a synergistic induction of CXCL4 compared with long-chain polyphosphates or LPS alone (Figure 2A). This synergy was also evident at the transcriptional level with higher CXCL4 mRNA abundance in macrophages co-treated with long-chain polyphosphates and LPS (Figure 2B). Next, we studied whether polyphosphates mediate CXCL4 induction also through TLR4. We examined the amount of CXCL4 released by polyphosphate- and LPS-treated macrophages from MyD88$^{-/-}$ and TRIF$^{-/-}$ mice side-by-side with wild type. Long-chain polyphosphates alone did not require MyD88 or TRIF for the induction of CXCL4, suggesting that polyphosphates are not ligands of TLRs (Figure 2C). There was a mild trend towards lower CXCL4 release in macrophages from MyD88$^{-/-}$ mice treated with LPS alone or together with long-chain polyphosphates when compared to WT mice

(Figure 2C). In contrast, TRIF$^{-/-}$ macrophages seemed rather more responsive to the combination of LPS and long-chain polyphosphates. These findings fit with the concept that LPS activates CXCL4 gene expression mainly through the MyD88 pathway.

The phosphatidylinositol 3-kinase/Akt serine/threonine kinase (PI3K/Akt) pathway is downstream of MyD88 and is involved in regulation of inflammatory responses (29). It is activated or suppressed based on phosphorylation of key amino acid residues of Akt (28). Macrophages treated with long-chain polyphosphates showed substantial phosphorylation of Akt at threonine-308 (T308) in a time-dependent manner using a bead-based assay (Figure 2D). When macrophages were co-treated with either of two Akt inhibitors, Wortmannin or Ly294002, there was a marked reduction in the amount of CXCL4 released (Figures 2E, F). In another series of experiments, we observed that long-chain polyphosphates also augmented LPS-mediated phosphorylation of Akt at T308, as evident from the increased frequencies of CD11b$^+$F4/80$^+$ macrophages positive for p-Akt (T308) when compared to controls (controls: 1.57%; LPS: 14.1%; LPS + L-PolyP: 39.1%), as detected by flow cytometry (Figures 2G, H). These findings suggest that long-chain polyphosphates have a substantial impact on dysregulating immune responses by interacting with the PI3K/Akt pathway in macrophages.

Long-chain polyphosphates promote lung injury

To study the contribution of polyphosphates to inflammation and CXCL4 release *in vivo*, we injected polyphosphates into the trachea of C57BL/6J mice. Histopathological examination of mouse lungs after intratracheal long-chain polyphosphate challenge showed diffuse hypercellularity caused by accumulation of PMNs, hyaline membranes, and alveolar wall thickening consistent with pulmonary edema and acute lung injury (Figure 3A). The total protein content in bronchoalveolar lavage fluid (BALF) was also significantly higher in long-chain polyphosphate-treated mice compared to sham controls (Figure 3B), consistent with greater disruption of the endothelial-epithelial barrier.

Immunophenotyping showed relatively higher influx of Ly6G$^+$ PMNs and lower numbers of CD11c$^+$SiglecF$^+$ alveolar macrophages (AMs) in BALF after long-chain polyphosphate-induced lung injury compared to sham controls (Figures 3C–G). Consistent with *in vitro* findings, there was augmented presence of CXCL4 compared to controls (Figure 3H).

Based on these observations, we next analyzed whether the extent of lung injury correlated with polyphosphate chain length. Long-chain polyphosphates consistently mediated significantly greater lung injury compared with medium-chain polyphosphates (M-PolyP; mean polymer length of ~240 P$_i$),
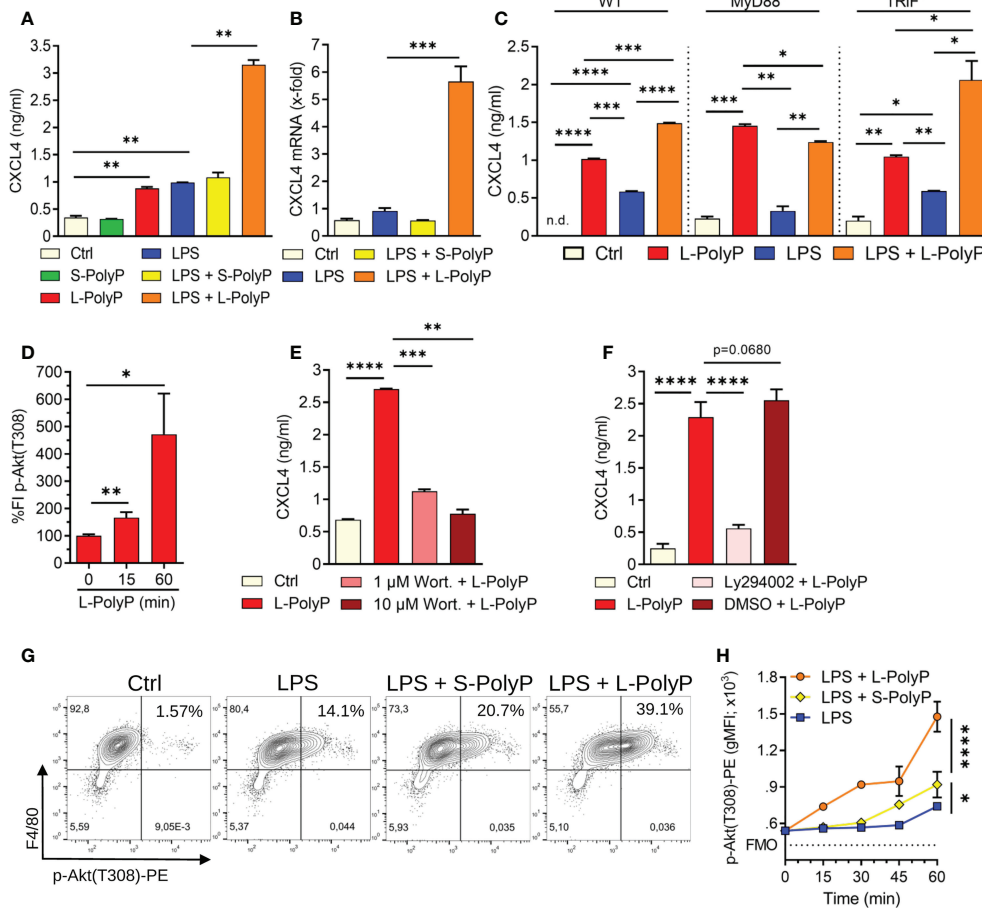
FIGURE 2

Polyphosphates regulate CXCL4 through PI3K/Akt signaling in macrophages. **(A)** CXCL4 release from C57BL/6J wild type macrophages (PEMs) after incubation with long-chain or short-chain polyphosphates ± LPS (100 ng/ml), Ctrl: resting control cells, 24 h, ELISA. **(B)** CXCL4 mRNA expression in macrophages (PEMs) after polyphosphates ± LPS, 24 h, RT-PCR. **(C)** CXCL4 release from macrophages (BMDMs) of wild type (WT), MyD88$^{-/-}$ and TRIF$^{-/-}$ mice, 24 h, ELISA. **(D)** Relative quantification of phosphorylated Akt (threonine-308) in macrophages (BMDMs) at 0-60 min after long-chain polyphosphates. The values of fluorescence intensities (FI) were normalized to controls (0 min), bead-based assay. **(E)** CXCL4 release from polyphosphate-stimulated macrophages (BMDMs) co-treated with the Akt inhibitor, Wortmannin, 24 h, ELISA. **(F)** CXCL4 release from macrophages (BMDMs) co-treated with the Akt inhibitor, Ly294002 (stock was dissolved in DMSO), 24 h, ELISA. **(G)** Contour plots of phospho-Akt in F4/80$^+$ macrophages (BMDMs) after activation with short/long-chain polyphosphates and LPS, 60 min, flow cytometry. **(H)** Geometric mean fluorescence intensities (gMFI) of pooled data (n=4/condition) as in frame G. Data are presented as mean ± SEM; *p < 0.05; **p < 0.01; ***p < 0.001; ****p < 0.0001; n.d.: not detectable.

short-chain polyphosphates, and controls, as demonstrated by the highest albumin content, highest influx of PMNs, and greater induction of CXCL4 in BALF (Figures 3I–K).

We next sought to understand the role of CXCL4 in long-chain polyphosphate-mediated lung injury. As blocking antibodies and knockout mice for CXCL4 were not available, we performed studies testing recombinant CXCL4 administration. While recombinant CXCL4 alone caused a non-significant trend of PMN influx (4.2 ± 0.6% vs. 1.0 ± 0.1%) to the lungs compared to controls, we observed no synergistic effects with long-chain polyphosphates in terms of alveolar/endothelial barrier disruption (total protein in BALF) and numbers of alveolar macrophages and PMNs

(Supplementary Figure 1A). When knockout mice for the promiscuous CXCL4 receptor, CXCR3, were studied, the only difference in the acute phase of polyphosphate-induced lung injury was a lower frequency of alveolar macrophages (Supplementary Figure 1B). Together, these data suggest a redundant role for CXCL4 in the severity of polyphosphate-induced acute lung injury.

To extrapolate our findings to the human lung, we assessed the basal cellular expression of CXCL4 and CXCR3 in a publicly available normal lung single cell transcriptomic dataset. This analysis showed low basal mRNA expression of CXCL4 in macrophages. On the other hand, CXCR3 expression was only abundant in plasmacytoid dendritic cells (pDCs) and T cells
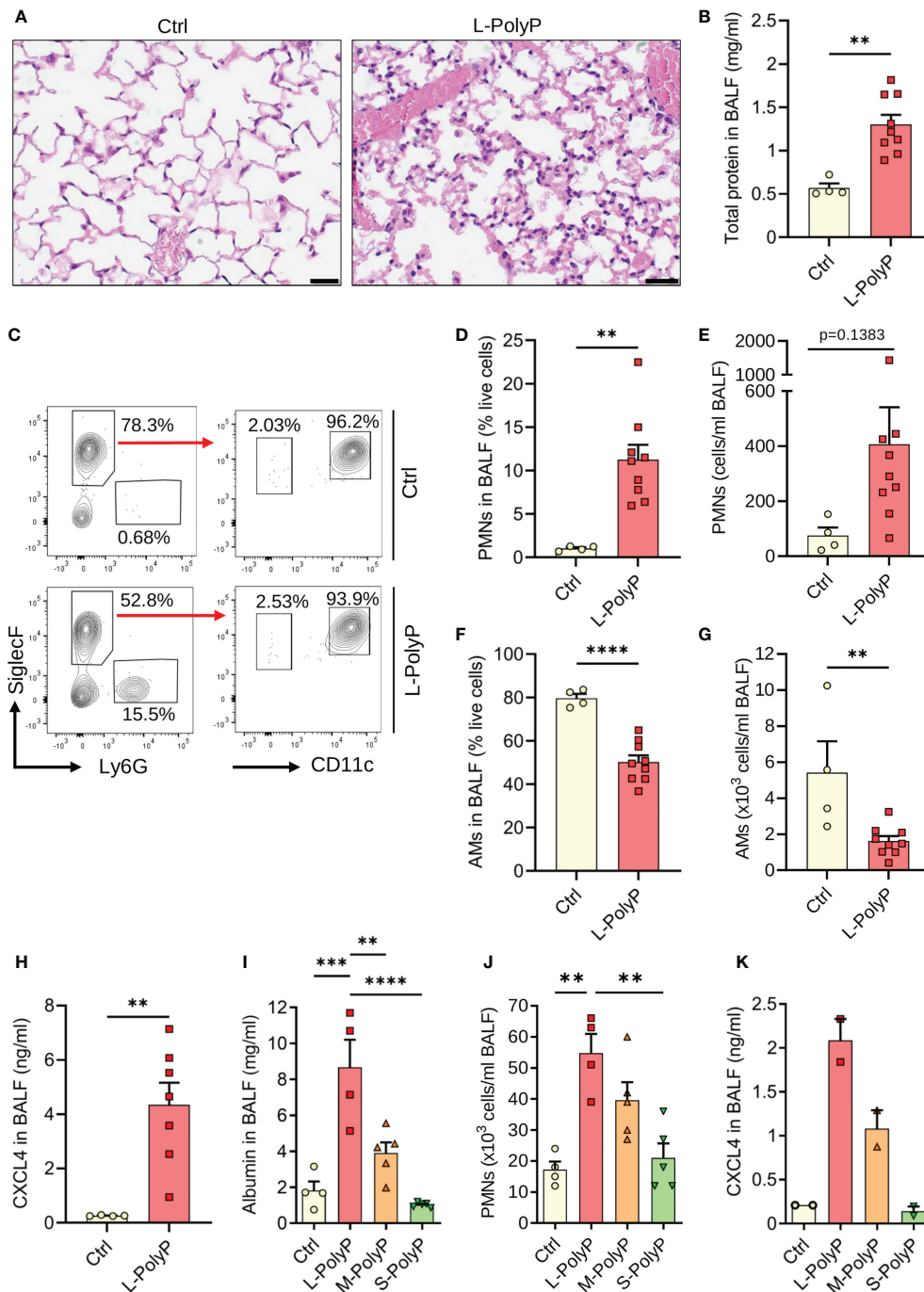
FIGURE 3

Long-chain polyphosphates cause lung injury. **(A)** Lung sections of C57BL/6J wild type mice obtained 8 h after intratracheal (i.t.) administration of long-chain polyphosphates (40 µl at 20 mM/mouse). Sham control mice (Ctrl) received PBS (40 µl/mouse i.t.), H&E staining, scale bar: 20 µm. **(B)** Total protein in bronchoalveolar lavage fluids (BALF) after long-chain polyphosphates or sham control treatment, 8 h, BCA assay. **(C)** Polyphosphate-induced lung injury in wild type mice compared to sham controls, 8 h. Representative contour plots of Ly6G$^+$ polymorphonuclear neutrophils (PMNs), CD11c$^+$SiglecF$^+$ alveolar macrophages and SiglecF$^+$Ly6G$^-$CD11c$^-$ eosinophils in BALF samples are shown, flow cytometry. **(D, E)** PMN frequencies and absolute numbers from mice as in frame C. **(F, G)** Frequencies and absolute numbers of alveolar macrophages (AMs) from mice as in frame C. **(H)** CXCL4 in BALF of mice as in frame C. **(I)** Albumin in BALF of wild type mice administered i.t. with long-chain (L), medium-chain (M), short-chain (S) polyphosphates, or sham controls, 8 h, ELISA. **(J)** PMN numbers in BALF from mice as in frame I, manual count. **(K)** CXCL4 in BALF from mice as described in frame I. Data are presented as mean ± SEM; *p < 0.05; **p < 0.01; ***p < 0.001; ****p < 0.0001.

(Supplementary Figure 2). Since T cells and pDCs are not many in number during the early phase of lung injury, this may explain some of the observed results.

Cross-talk between long-chain polyphosphates and C5a in lung injury

Complement activation plays an important part in the host response to pathogens. Polyphosphates can suppress the classical and terminal complement pathways (7, 30). The complement anaphylatoxin, C5a, and interaction with its receptor, C5aR1, drive the pathophysiology of ALI (16, 17, 19). To investigate the potential cross-talk of polyphosphates with C5a regarding the severity of lung injury and CXCL4 release, we combined polyphosphate administration with our reported model of C5a-induced lung injury (16). A lower dose of C5a (100 ng/mouse instead of 500 ng/ml) was used to better uncover any permissive effects of polyphosphates. Using this approach, we observed a synergistic increase in albumin content in BALF from mice that were co-administered both rmC5a and long-chain polyphosphates compared with each alone (Figure 4A). In addition, there was abundant release of CXCL4 in BALF from mice that received a combination of rmC5a and polyphosphates compared with mice that received only polyphosphates or rmC5a, and sham controls (Figure 4B). The effects of polyphosphates on C5a-mediated lung injury were partly explained by the elevated expression of C5aR1 on myeloid cells from long-chain polyphosphate-treated mice compared to controls (Figure 4C). The geometric mean fluorescence intensity (gMFI) values for C5aR1 were higher in PMNs and alveolar macrophages from long-chain polyphosphate challenged mice compared to controls, though this difference was statistically significant only for alveolar macrophages (Figures 4D, E). The synergistic action of polyphosphates and C5a was further confirmed by studies using C5aR1$^{-/-}$ mice, where we observed a significant reduction in albumin leakage and suppressed liberation of CXCL4 in long-chain polyphosphate-treated C5aR1$^{-/-}$ mice compared with C57BL/6J wild type (WT) mice (Figures 4F, G). In line with this concept, C5a generation was found to be increased in lung lysates and BALF of wild type mice treated intratracheally with long-chain polyphosphates as studied by tandem immunoprecipitation and western blotting (Figures 4H–J).

Collectively, these findings support that polyphosphate-mediated lung injury is amplified through a C5a-dependent mechanism.

Discussion

In this study, we have established that polyphosphates acutely induce the typical signs of experimental lung injury

(31), when administered to the airways of healthy mice. Polyphosphate concentrations are elevated in the blood and extracellular fluids during bacterial infection (8), although it is unknown if such polyphosphates are actively secreted or passively released. Bacterial pneumonia is a major cause that precipitates the development of ALI/ARDS in clinical settings (32). Hence, polyphosphates could represent a pathogenic mechanism linking bacterial infection to the development of ALI/ARDS. In addition, complement activation and C5a-mediated dysregulation of the inflammatory response are culprits in the pathophysiology of ARDS (16, 17, 19, 33). Elevated C5a is found in the lung epithelial lining fluid of ARDS patients, which resolves after recovery (34). In septic primates, anti-C5a antibodies protect against decreased oxygenation, pulmonary edema, and lethality (35). Our findings suggest that polyphosphates aggravate the influx of PMNs and destruction of the lung barrier caused by C5a (Figure 4), whereas no synergistic effect of the polyphosphates and CXCL4 combination was observed for these endpoints (Supplementary Figure 1).

Moreover, we found that polyphosphates promote the generation of C5a in the lung and that C5aR1$^{-/-}$ mice are partly protected from the deleterious effects of polyphosphates. Interestingly, we and others have previously reported that C5a induces PI3K/Akt signaling in macrophages and that in vivo inhibition of PI3K/Akt by wortmannin greatly inhibits C5a-induced acute lung injury (16, 36, 37). Since we show in this study that polyphosphates also induce PI3K signaling, the synergy of polyphosphates and C5a could be explained by their additive effects on the activation of the PI3K/Akt pathway. Although not formally investigated, the co-presence of intrapulmonary long-chain polyphosphates and C5a can be considered highly likely in bacterial pneumonia. C5a can originate from classical, lectin, and alternative pathway activation during bacterial infection (19). Since polyphosphates inhibit the classical pathway (by accelerating the effects of C1-inhibitor) and the lectin pathway (30), such polyphosphate-induced generation of C5a might arise from the alternative pathway. In addition, polyphosphates decrease the terminal complement pathway by binding to the C5b,C6 complex (7). Our findings suggest that polyphosphates are not global inhibitors of complement activation, but rather can act bidirectionally as either an inhibitor or inducer depending on the context.

We have identified that the pathophysiological potency of polyphosphates increases with chain length, which demonstrates the distinctive roles of short-chain polyphosphates from platelets and long-chain polyphosphates from bacteria. It is tempting to speculate that a chain length greater than P_i70 could be needed because polyphosphates may simultaneously bind two proteins, which are then brought into spatial proximity by a long polyphosphate chain. It remains enigmatic whether bacterial
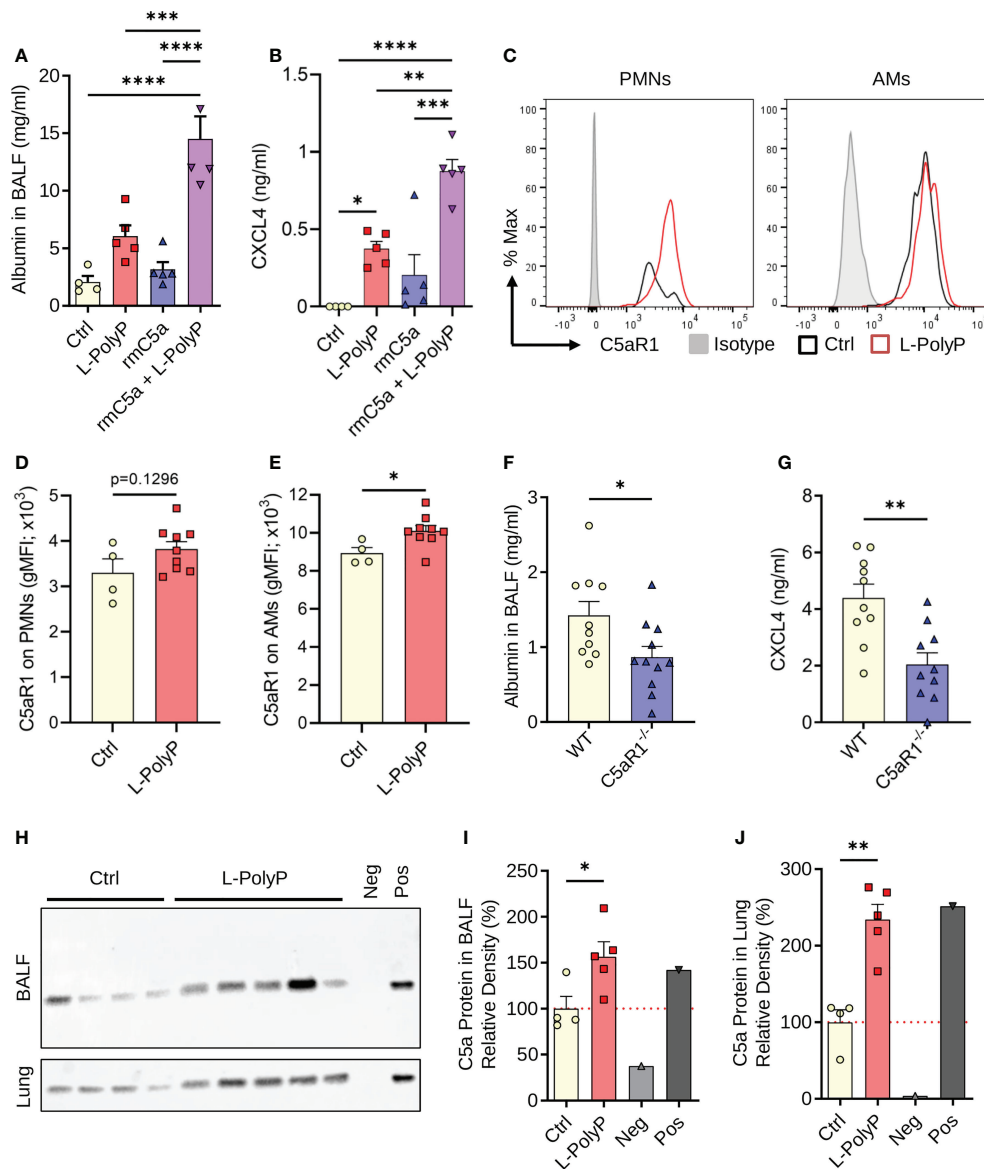
FIGURE 4

Polyphosphates synergize with C5a in lung injury. **(A)** Albumin in BALF of C57BL/6J wild type mice after long-chain polyphosphate-induced lung injury (40 µl at 20 mM/mouse) ± recombinant mouse C5a (100 ng/mouse i.t.), 8 h, ELISA. Sham control mice (Ctrl) received PBS (40 µl/mouse i.t.). **(B)** CXCL4 in BALF from mice as in frame A, ELISA. **(C)** C5aR1 histograms pre-gated on PMNs or alveolar macrophages (AMs) from representative mice after polyphosphate-induced lung injury or sham treated controls. **(D, E)** C5aR1 surface expression as geometric mean fluorescence intensities on PMNs and AMs from mice as in frame C. **(F)** Alveolar albumin in wild type (WT) and C5aR1$^{-/-}$ mice after long-chain polyphosphate-induced lung injury (40 µl at 20 mM/mouse), 8 h, ELISA. **(G)** CXCL4 in BALF from WT and C5aR1$^{-/-}$ mice as in frame F, 8 h, ELISA. **(H)** Western blots of immunoprecipitated C5a from BALF and lung lysates obtained 6 h after long-chain polyphosphate-induced lung injury (n=5) or sham treatment (Ctrl; n=4) in WT mice. Recombinant mouse C5a (~9 kDa, 10 ng) was directly applied to the lane as a positive control (Pos). The negative control (Neg) contained Protein A agarose beads and Laemmli buffer. **(I, J)** C5a abundance in BALF and lung as expressed by densitometry of bands shown in frame H, normalized to sham treatment. Data are presented as mean ± SEM; *p < 0.05; **p < 0.01; ***p < 0.001; ****p < 0.0001.

polyphosphates are recognized by yet unidentified pattern-recognition sensors or if their biological activities are an integrated result of manifold interactions with several positively charged host proteins. Our finding that polyphosphates remained fully capable of inducing CXCL4 in

MyD88$^{-/-}$ and TRIF$^{-/-}$ macrophages suggests that Toll-like receptors are not involved (Figure 2C). We could not confirm a requirement for P2Y1 as a polyphosphate sensor in macrophages (8), although P2Y1 may transmit some effects in non-immune cells (27, 38).

While a classical ligand-receptor relationship remains unidentified, we uncover that polyphosphates activate PI3K/Akt signaling in macrophages. This expands earlier reports that polyphosphates recruit Akt and mTOR in human endothelial cells and breast cancer cells (5, 39). Moreover, we have shown that polyphosphates directly bind several human proteins associated with the PI3K/Akt pathway (40).

While the major constitutive sources of CXCL4 are platelets and megakaryocytes, CXCL4 gene expression is also inducible in mononuclear phagocytes and their hematopoietic precursors (41–46). Macrophages are also target cells for CXCL4 effects. CXCL4 prevents macrophage apoptosis, promotes phagocytosis, and provokes the formation of reactive oxygen species, but lacks any chemotactic effect in these cells (47). In defined pathologies, CXCL4-activated macrophages can display distinct phenotypic and functional characteristics such as production of CXCL2 and PDGF-BB, or loss of the hemoglobin-haptoglobin scavenger receptor, CD163 (48–51).

Polyphosphates mediate the release of their binding partner, CXCL4 (12), although both appeared not to synergize in fueling a more severe lung injury in our studies. Suggesting a dispensable role of CXCL4, we found that total protein leakage and PMN numbers in BALF are not different with co-administration of recombinant CXCL4 or in mice deficient in CXCR3. Of note, interpretation of findings in CXCR3$^{-/-}$ mice is ambiguous because CXCL4, CXCL9, CXCL10 and CXCL11 all signal through CXCR3 (52). Even more complicating, CCR1 has recently been proposed as an alternative receptor for CXCL4 in a human monocytic cell line (53). Interestingly, CXCL4$^{-/-}$ mice show improved histopathologic scores and lower total protein in BALF, albeit unchanged PMN numbers in acid aspiration-induced lung injury (54). Furthermore, CXCL4$^{-/-}$ mice have diminished viral clearance and decreased PMN influx in the early stage of H1N1 influenza virus infection, which is followed by more severe lymphocytic lung pathology and higher mortality at later stages (55). In experimental bacterial pneumonia caused by *Pseudomonas aeruginosa*, CXCL4$^{-/-}$ mice show defective bacterial clearance, more severe endothelial/epithelial permeability disturbances, reduced PMN accumulation in the lungs, and reduced blood platelet-neutrophil interactions (56). Transgenic mice overexpressing human CXCL4 are protected from early lethality (16-48 hours) after LPS-induced endotoxic shock (57). Thus, a pathophysiologic relevance of CXCL4 in infection and lung disease is supported by the literature, although we could not directly confirm this with our approach and at the early 8 hour time point studied. Another limitation of our study is that (in the absence of CXCL4-reporter mice) we could not determine the cellular sources of CXCL4 during lung injury *in vivo*, which could include platelet/megakaryocytes and mononuclear phagocytes.

In our experience, the activity profiles of polyphosphates are unique, specific and context dependent. Polyphosphates alone are not broadly proinflammatory or directly cytotoxic for macrophages *in vitro* (8). In our laboratory, we routinely use polyphosphate-induced CXCL4 release as a positive control and convenient endpoint for validation in many studies.

We propose the general concept that bacteria-derived, long-chain polyphosphates represent an immune evasion strategy which misdirects inflammation to cause tissue damage and prevent efficient pathogen clearance. Gram-negative bacteria encode genes for the enzyme, polyphosphatekinase (PPK), to synthesize polyphosphates from ATP. While gram-positive bacteria can also produce polyphosphates, no PPK homologs exist and alternate enzymatic machineries await identification. Instead of targeting polyphosphate synthesis in bacteria, we propose that administration of recombinant polyphosphatases could be of broad therapeutic value in sepsis and ALI/ARDS from both gram-negative and gram-positive bacteria. To further validate this potential approach, experimental studies of ARDS induced by infections with live bacteria will be needed in the future.

Data availability statement

The datasets presented in this study can be found in online repositories. The names of the repository/repositories and accession number(s) can be found in the article/Supplementary Material.

Ethics statement

The animal study was reviewed and approved by The State Investigation Office of Rhineland-Palatinate and The Institutional Animal Care and Use Committee (IACUC) of Boston University.

Author contributions

JR, SW, AS and KB designed and performed experiments, and analyzed data. CR provided MyD88$^{-/-}$ and TRIF$^{-/-}$ mice. MB and JR wrote the manuscript, which was edited by SW, AS and CR. MB conceived and supervised the study, designed experiments, interpreted data, and provided funding. All authors contributed to the article and approved the submitted version.

Funding

Acknowledgments

Conflict of interest

The authors declare that the research was conducted in the absence of any commercial or financial relationships that could be construed as a potential conflict of interest.

Publisher's note

All claims expressed in this article are solely those of the authors and do not necessarily represent those of their affiliated organizations, or those of the publisher, the editors and the reviewers. Any product that may be evaluated in this article, or claim that may be made by its manufacturer, is not guaranteed or endorsed by the publisher.

Supplementary material

The Supplementary Material for this article can be found online at: https://www.frontiersin.org/articles/10.3389/fimmu.2022.980733/full#supplementary-material

References

1. Rao NN, Gómez-García MR, Kornberg A. Inorganic polyphosphate: Essential for growth and survival. *Annu Rev Biochem* (2009) 78:605–47. doi: 10.1146/annurev.biochem.77.083007.093039

2. Smith SA, Choi SH, Davis-Harrison R, Huyck J, Boettcher J, Rienstra CM, et al. Polyphosphate exerts differential effects on blood clotting, depending on polymer size. *Blood* (2010) 116(20):4353–9. doi: 10.1182/blood-2010-01-266791

3. Gray MJ, Wholey WY, Wagner NO, Cremers CM, Mueller-Schickert A, Hock NT, et al. Polyphosphate is a primordial chaperone. *Mol Cell* (2014) 53 (5):689–99. doi: 10.1016/j.molcel.2014.01.012

4. Xie L, Jakob U. Inorganic polyphosphate, a multifunctional polyanionic protein scaffold. *J Biol Chem* (2019) 294(6):2180–90. doi: 10.1074/jbc.REV118.002808

5. Wang L, Fraley CD, Faridi J, Kornberg A, Roth RA. Inorganic polyphosphate stimulates mammalian tor, a kinase involved in the proliferation of mammary cancer cells. *Proc Natl Acad Sci U S A* (2003) 100(20):11249–54. doi: 10.1073/pnas.1534805100

6. Dahl JU, Gray MJ, Bazopoulou D, Beaufay F, Lempart J, Koenigsknecht MJ, et al. The anti-inflammatory drug mesalamine targets bacterial polyphosphate accumulation. *Nat Microbiol* (2017) 2:16267. doi: 10.1038/nmicrobiol.2016.267

7. Wat JM, Foley JH, Krisinger MJ, Ocariza LM, Lei V, Wasney GA, et al. Polyphosphate suppresses complement *Via* the terminal pathway. *Blood* (2014) 123(5):768–76. doi: 10.1182/blood-2013-07-515726

8. Roewe J, Stavrides G, Strueve M, Sharma A, Marini F, Mann A, et al. Bacterial polyphosphates interfere with the innate host defense to infection. *Nat Commun* (2020) 11(1):4035. doi: 10.1038/s41467-020-17639-x

9. Suess PM, Chinea LE, Pilling D, Gomer RH. Extracellular polyphosphate promotes macrophage and fibrocyte differentiation, inhibits leukocyte proliferation, and acts as a chemotactic agent for neutrophils. *J Immunol* (2019) 203(2):493–9. doi: 10.4049/jimmunol.1801559

10. Rijal R, Cadena LA, Smith MR, Carr JF, Gomer RH. Polyphosphate is an extracellular signal that can facilitate bacterial survival in eukaryotic cells. *Proc Natl Acad Sci U S A* (2020) 117(50):31923–34. doi: 10.1073/pnas.2012009117

11. Harada K, Shiba T, Doi K, Morita K, Kubo T, Makihara Y, et al. Inorganic polyphosphate suppresses lipopolysaccharide-induced inducible nitric oxide synthase (Inos) expression in macrophages. *PLoS One* (2013) 8(9):e74650. doi: 10.1371/journal.pone.0074650

12. Brandt S, Krauel K, Jaax M, Renné T, Helm CA, Hammerschmidt S, et al. Polyphosphates form antigenic complexes with platelet factor 4 (Pf4) and enhance Pf4-binding to bacteria. *Thromb Haemost* (2015) 114(6):1189–98. doi: 10.1160/th15-01-0062

13. Lasagni L, Francalanci M, Annunziato F, Lazzeri E, Giannini S, Cosmi L, et al. An alternatively spliced variant of Cxcr3 mediates the inhibition of endothelial cell growth induced by ip-10, mig, and I-tac, and acts as functional receptor for platelet factor 4. *J Exp Med* (2003) 197(11):1537–49. doi: 10.1084/jem.20021897

14. Kowalska MA, Rauova L, Poncz M. Role of the platelet chemokine platelet factor 4 (Pf4) in hemostasis and thrombosis. *Thromb Res* (2010) 125(4):292–6. doi: 10.1016/j.thromres.2009.11.023

15. Vandercappellen J, Van Damme J, Struyf S. The role of the cxc chemokines platelet factor-4 (Cxcl4/Pf-4) and its variant (Cxcl4l1/Pf-4var) in inflammation, angiogenesis and cancer. *Cytokine Growth Factor Rev* (2011) 22(1):1–18. doi: 10.1016/j.cytogfr.2010.10.011

16. Russkamp NF, Ruemmler R, Roewe J, Moore BB, Ward PA, Bosmann M. Experimental design of complement component 5a-induced acute lung injury (C5a-ali): A role of cc-chemokine receptor type 5 during immune activation by anaphylatoxin. *FASEB J* (2015) 29(9):3762–72. doi: 10.1096/fj.15-271635

17. Bosmann M, Grailer JJ, Ruemmler R, Russkamp NF, Zetoune FS, Sarma JV, et al. Extracellular histones are essential effectors of C5ar- and C5l2-mediated tissue damage and inflammation in acute lung injury. *FASEB J* (2013) 27(12):5010–21. doi: 10.1096/fj.13-236380

18. Bosmann M, Russkamp NF, Strobl B, Roewe J, Balouzian L, Pache F, et al. Interruption of macrophage-derived il-27(P28) production by il-10 during sepsis requires Stat3 but not Socs3. *J Immunol* (2014) 193(11):5668–77. doi: 10.4049/jimmunol.1302280

19. Bosmann M, Ward PA. Role of C3, C5 and anaphylatoxin receptors in acute lung injury and in sepsis. *Adv Exp Med Biol* (2012) 946:147–59. doi: 10.1007/978-1-4614-0106-3_9

20. Livak KJ, Schmittgen TD. Analysis of relative gene expression data using real-time quantitative pcr and the 2(-delta delta C(T)) method. *Methods* (2001) 25(4):402–8. doi: 10.1006/meth.2001.1262

21. Cui W, Taub DD, Gardner K. Qprimerdepot: A primer database for quantitative real time pcr. *Nucleic Acids Res* (2007) 35:D805–9. doi: 10.1093/nar/gkl767

22. Smith SA, Baker CJ, Gajsiewicz JM, Morrissey JH. Silica particles contribute to the procoagulant activity of DNA and polyphosphate isolated using commercial kits. *Blood* (2017) 130(1):88–91. doi: 10.1182/blood-2017-03-772848

23. Travaglini KJ, Nabhan AN, Penland L, Sinha R, Gillich A, Sit RV, et al. A molecular cell atlas of the human lung from single-cell rna sequencing. *Nature* (2020) 587(7835):619–25. doi: 10.1038/s41586-020-2922-4

24. Travaglini KJ, Nabhan AN, Penland L, Sinha R, Gillich A, Sit RV, et al. *Processed data from cellxgene for: A molecular cell atlas of the human lung from single-cell rna sequencing* (2020) (Accessed 23 March 2022).

25. Korsunsky I, Millard N, Fan J, Slowikowski K, Zhang F, Wei K, et al. Fast, sensitive and accurate integration of single-cell data with harmony. *Nat Methods* (2019) 16(12):1289–96. doi: 10.1038/s41592-019-0619-0

26. Satija R, Farrell JA, Gennert D, Schier AF, Regev A. Spatial reconstruction of single-cell gene expression data. *Nat Biotechnol* (2015) 33(5):495–502. doi: 10.1038/nbt.3192

27. Dinarvand P, Hassanian SM, Qureshi SH, Manithody C, Eissenberg JC, Yang L, et al. Polyphosphate amplifies proinflammatory responses of nuclear proteins through interaction with receptor for advanced glycation end products and P2y1 purinergic receptor. *Blood* (2014) 123(6):935–45. doi: 10.1182/blood-2013-09-529602

28. Laird MH, Rhee SH, Perkins DJ, Medvedev AE, Piao W, Fenton MJ, et al. Tlr4/Myd88/Pi3k interactions regulate Tlr4 signaling. *J Leukoc Biol* (2009) 85(6):966–77. doi: 10.1189/jlb.1208763

29. Gelman AE, LaRosa DF, Zhang J, Walsh PT, Choi Y, Sunyer JO, et al. The adaptor molecule Myd88 activates pi-3 kinase signaling in Cd4+ T cells and enables cpg oligodeoxynucleotide-mediated costimulation. *Immunity* (2006) 25(5):783–93. doi: 10.1016/j.immuni.2006.08.023

30. Wijeyewickrema LC, Lameignere E, Hor L, Duncan RC, Shiba T, Travers RJ, et al. Polyphosphate is a novel cofactor for regulation of complement by a serpin, C1 inhibitor. *Blood* (2016) 128(13):1766–76. doi: 10.1182/blood-2016-02-699561

31. Matute-Bello G, Downey G, Moore BB, Groshong SD, Matthay MA, Slutsky AS, et al. An official American thoracic society workshop report: Features and measurements of experimental acute lung injury in animals. *Am J Respir Cell Mol Biol* (2011) 44(5):725–38. doi: 10.1165/rcmb.2009-0210ST

32. Matthay MA, Ware LB, Zimmerman GA. The acute respiratory distress syndrome. *J Clin Invest* (2012) 122(8):2731–40. doi: 10.1172/JCI60331

33. Mulligan MS, Schmid E, Beck-Schimmer B, Till GO, Friedl HP, Brauer RB, et al. Requirement and role of C5a in acute lung inflammatory injury in rats. *J Clin Invest* (1996) 98(2):503–12. doi: 10.1172/JCI118818

34. Robbins RA, Russ WD, Rasmussen JK, Clayton MM. Activation of the complement system in the adult respiratory distress syndrome. *Am Rev Respir Dis* (1987) 135(3):651–8. doi: 10.1164/arrd.1987.135.3.651

35. Stevens JH, O'Hanley P, Shapiro JM, Mihm FG, Satoh PS, Collins JA, et al. Effects of anti-C5a antibodies on the adult respiratory distress syndrome in septic primates. *J Clin Invest* (1986) 77(6):1812–6. doi: 10.1172/JCI112506

36. Bosmann M, Patel VR, Russkamp NF, Pache F, Zetoune FS, Sarma JV, et al. Myd88-dependent production of il-17f is modulated by the anaphylatoxin C5a *Via* the akt signaling pathway. *FASEB J* (2011) 25(12):4222–32. doi: 10.1096/fj.11-191205

37. Bosmann M, Sarma JV, Atefi G, Zetoune FS, Ward PA. Evidence for anti-inflammatory effects of C5a on the innate il-17a/Il-23 axis. *FASEB J* (2012) 26(4):1640–51. doi: 10.1096/fj.11-199216

38. Holmstrom KM, Marina N, Baev AY, Wood NW, Gourine AV, Abramov AY. Signalling properties of inorganic polyphosphate in the mammalian brain. *Nat Commun* (2013) 4:1362. doi: 10.1038/ncomms2364

39. Hassanian SM, Dinarvand P, Smith SA, Rezaie AR. Inorganic polyphosphate elicits pro-inflammatory responses through activation of the mammalian target of rapamycin complexes 1 and 2 in vascular endothelial cells. *J Thromb Haemost* (2015) 13(5):860–71. doi: 10.1111/jth.12899

40. Krenzlin V, Roewe J, Strueve M, Martinez-Negro M, Sharma A, Reinhardt C, et al. Bacterial-type long-chain polyphosphates bind human proteins in the phosphatidylinositol signaling pathway. *Thromb Haemost* (2022). doi: 10.1055/s-0042-1751280

41. Schaffner A, Rhyn P, Schoedon G, Schaer DJ. Regulated expression of platelet factor 4 in human monocytes—role of pars as a quantitatively important monocyte activation pathway. *J Leukoc Biol* (2005) 78(1):202–9. doi: 10.1189/jlb.0105024

42. Maier M, Geiger EV, Henrich D, Bendt C, Wutzler S, Lehnert M, et al. Platelet factor 4 is highly upregulated in dendritic cells after severe trauma. *Mol Med* (2009) 15(11-12):384–91. doi: 10.2119/molmed.2009.00074

43. Maier M, Wutzler S, Bauer M, Trendafilov P, Henrich D, Marzi I. Altered gene expression patterns in dendritic cells after severe trauma: Implications for systemic inflammation and organ injury. *Shock* (2008) 30(4):344–51. doi: 10.1097/SHK.0b013e3181673eb4

44. Pertuy F, Aguilar A, Strassel C, Eckly A, Freund JN, Duluc I, et al. Broader expression of the mouse platelet factor 4-cre transgene beyond the megakaryocyte lineage. *J Thromb Haemost* (2015) 13(1):115–25. doi: 10.1111/jth.12784

45. Abram CL, Roberge GL, Hu Y, Lowell CA. Comparative analysis of the efficiency and specificity of myeloid-cre deleting strains using Rosa-eyfp reporter mice. *J Immunol Methods* (2014) 408:89–100. doi: 10.1016/j.jim.2014.05.009

46. Lyras EM, Zimmermann K, Wagner LK, Dorr D, Klose CSN, Fischer C, et al. Tongue immune compartment analysis reveals spatial macrophage heterogeneity. *Elife* (2022) 11:e77490. doi: 10.7554/eLife.77490

47. Pervushina O, Scheuerer B, Reiling N, Behnke L, Schroder JM, Kasper B, et al. Platelet factor 4/Cxcl4 induces phagocytosis and the generation of reactive oxygen metabolites in mononuclear phagocytes independently of gi protein activation or intracellular calcium transients. *J Immunol* (2004) 173(3):2060–7. doi: 10.4049/jimmunol.173.3.2060

48. Gleissner CA, Shaked I, Erbel C, Bockler D, Katus HA, Ley K. Cxcl4 downregulates the atheroprotective hemoglobin receptor Cd163 in human macrophages. *Circ Res* (2010) 106(1):203–11. doi: 10.1161/CIRCRESAHA.109.199505

49. Gleissner CA. Macrophage phenotype modulation by Cxcl4 in atherosclerosis. *Front Physiol* (2012) 3:1. doi: 10.3389/fphys.2012.00001

50. Hwaiz R, Rahman M, Zhang E, Thorlacius H. Platelet secretion of Cxcl4 is Rac1-dependent and regulates neutrophil infiltration and tissue damage in septic lung damage. *Br J Pharmacol* (2015) 172(22):5347–59. doi: 10.1111/bph.13325

51. van der Kroef M, Carvalheiro T, Rossato M, de Wit F, Cossu M, Chouri E, et al. Cxcl4 triggers monocytes and macrophages to produce pdgf-bb, culminating in fibroblast activation: Implications for systemic sclerosis. *J Autoimmun* (2020) 111:102444. doi: 10.1016/j.jaut.2020.102444

52. Kuo PT, Zeng Z, Salim N, Mattarollo S, Wells JW, Leggatt GR. The role of Cxcr3 and its chemokine ligands in skin disease and cancer. *Front Med (Lausanne)* (2018) 5:271. doi: 10.3389/fmed.2018.00271

53. Fox JM, Kausar F, Day A, Osborne M, Hussain K, Mueller A, et al. Cxcl4/Platelet factor 4 is an agonist of Ccr1 and drives human monocyte migration. *Sci Rep* (2018) 8(1):9466. doi: 10.1038/s41598-018-27710-9

54. Bdeir K, Gollomp K, Stasiak M, Mei J, Papiewska-Pajak I, Zhao G, et al. Platelet-specific chemokines contribute to the pathogenesis of acute lung injury. *Am J Respir Cell Mol Biol* (2017) 56(2):261–70. doi: 10.1165/rcmb.2015-0245OC

55. Guo L, Feng K, Wang YC, Mei JJ, Ning RT, Zheng HW, et al. Critical role of Cxcl4 in the lung pathogenesis of influenza (H1n1) respiratory infection. *Mucosal Immunol* (2017) 10(6):1529–41. doi: 10.1038/mi.2017.1

56. Yue L, Pang Z, Li H, Yang T, Guo L, Liu L, et al. Cxcl4 contributes to host defense against acute pseudomonas aeruginosa lung infection. *PLoS One* (2018) 13(10):e0205521. doi: 10.1371/journal.pone.0205521

57. Kowalska MA, Mahmud SA, Lambert MP, Poncz M, Slungaard A. Endogenous platelet factor 4 stimulates activated protein c generation *in vivo* and improves survival after thrombin or lipopolysaccharide challenge. *Blood* (2007) 110(6):1903–5. doi: 10.1182/blood-2007-03-081901